Spin−Orbit Splittings in Mg^+−Neutral Complexes

Spiridoula Matsika and Russell M. Pitzer*

Department of Chemistry, The Ohio State University, 100 West 18th Avenue, Columbus, Ohio 43210

Received: October 31, 1997; In Final Form: December 19, 1997

Potential energy curves for the $X^2\Sigma^+_{1/2}$, $A^2\Pi_{1/2,3/2}$, and $B^2\Sigma^+_{1/2}$ states of the Mg^+−RG type complexes (where RG = Ar, Xe) were generated using relativistic spin−orbit configuration-interaction calculations based on effective core potentials. The anomalous behavior of the spin−orbit splitting of the $A^2\Pi$ state has been investigated and explained as an effect of the mixing of rare-gas valence pπ orbital into the Mg^+ 3pπ orbital in the wave function of the complex. A similar mixing causes a different behavior for the Mg^+−CO_2 complex, and this has also been investigated.

1. Introduction

Several complexes of metal ions with neutral atoms and molecules have been studied in the past both experimentally and theoretically. The studies have been focused on complexes with small molecules such as H_2O, NH_3, CO_2, or rare gases. In the particular case where the metal is an alkaline earth, it becomes easier to study these systems, so there have been quite interesting and extensive results.[1−17] The attractive interaction between the metal and the ligand in these complexes is mostly electrostatic and induction (charge-dipole, charge-quadrupole, charge-induced dipole). The ground-state $^2\Sigma^+$ arises from the ^{2}S state of the alkaline earth, while low-lying excited states arise from the ^{2}P state. When the valence electron is located in the pπ orbitals, a $^2\Pi$ state arises that is more strongly bound than the ground state because the unpaired electron, which does not contribute directly to the bonding, is concentrated along an axis perpendicular to the internuclear axis and away from the complexing species. The next excited state, $^2\Sigma^+$, is less bound than the ground state because the pσ valence electron density lies on the internuclear axis and increases the repulsion with the complexing species even more than the 3s density. None of the interaction energies is large enough to induce 3s−3p hybridization.

The complexes that we study in this work are Mg^+−Ar, Mg^+−Xe, and Mg^+−CO_2. Duncan and co-workers have studied Mg^+−RG,[4,6] Ca^+−RG,[5] where RG = Ar, Kr, Xe, and Mg^+−CO_2 using mass-selected photodissociation spectroscopy. They observed the $^2\Pi \leftarrow {}^2\Sigma$ transition and obtained vibrational constants, dissociation energies, and spin−orbit constants. For Mg^+−Ar they were able to obtain high-resolution rotationally resolved spectra[6] and therefore determine rotational constants and geometries.

Le Roy[16] did a further analysis of the above spectroscopic data using near-dissociation-theory techniques in order to improve the values of the dissociation energies of Mg^+−Ar and Mg^+−Kr.

Massick and Breckenridge report a dissociation energy for the ground state of Mg^+−Ar using the ionization potential of $Mg(3s3p^3P_0)$, and both the ionization potential and dissociation energy of $Mg(3s3p\ ^3P_0)Ar(^1S)^3\Pi_{0-}$.[17]

Bauschlicher, Partridge, and Sodupe have contributed much to the theoretical study of weakly bound complexes of Mg^+.[9−15] In recent work they performed calculations for Mg^+−Ar and Mg^+−Kr,[9] using large basis sets and performing CISD calculations where nine electrons were correlated. To take into account the Mg core-valence correlation and core polarization, they used the core-polarization potential approach suggested by Müller et al.[18] They have reported bond lengths, dissociation energies, excitation energies, Franck−Condon factors, oscillator strengths, and radiative lifetimes. The agreement with the experimental results is very good where comparison is possible. Since their calculations do not include relativistic effects, an important aspect of the problem concerning the spin−orbit splitting of the excited $^2\Pi$ state has not been treated. Earlier studies include that for Mg^+−CO_2[9] where the excitation energies and binding energies were calculated using the multireference configuration-interaction approach.

2. Methods

Relativistic calculations were performed. Since all-electron calculations are very expensive computationally, a common procedure is to use relativistic effective core potentials. In this method, the core electrons are replaced by a potential derived by all-electron relativistic atomic calculations and only the valence electrons are treated explicitly. Spin−orbit operators are generated simultaneously from the atomic calculations.[19,20]

In these calculations, the Mg^+ core consists of the two 1s electrons while the nine outermost electrons are considered to be in the valence region and are treated explicitly. For the rare gases the eight outermost electrons are treated explicitly. For C and O, four and six electrons are treated explicitly, respectively. The effective core potentials and spin−orbit operators are taken from Pacios et al.[21] except the ones used for Xe, which are from Nicklass et al.[22]

For the basis sets of C, O, and Ar, the optimized exponents are taken from Wallace et al.[23] while the exponents for Xe are taken from Nicklass et al.[22] The Ar basis set is augmented by adding diffuse functions taken from Kendall et al.[24] Diffuse basis functions are also added for O following Dunning's procedure.[24] For Mg^+ the exponents have been optimized using the ATMSCF program.[25] The way the contractions have been done in these basis sets[26] differs from the most common way. Traditionally, the contractions have been done in the same way as for all-electron basis sets: free the most diffuse primitive for each symmetry and let it orthogonalize itself to the SCF

* Corresponding author. E-mail: pitzer.3@osu.edu.

S1089-5639(98)00032-2 CCC: $15.00
Published on Web 02/07/1998

orbital of that symmetry. Core basis sets, however, describe pseudo-orbitals, and they all need to be small in the core region. The most diffuse primitives are not necessarily small in the core region (especially an s primitive, whose maximum is at the nucleus), and orthogonalizing to the SCF orbital does not change this property much, since the SCF orbital is small in the core region. The method we have tried here for doing the contractions is by using natural orbitals from uncontracted CISD calculations. The density matrices for p_x, p_y, and p_z were averaged where necessary. The CI calculation used for the Mg^+ basis set included all single excitations or simultaneous single excitation from 2s2p orbitals and single excitation from 3s3p orbitals in order to obtain contractions adapted to core-valence correlation. The same type of configurations were used in the complexes to describe the Mg core-valence correlation. For alkali and alkaline-earth atoms such as Mg, core-valence correlation is very important, and one needs to take this into consideration for accurate results. So appropriate basis functions need to be included as well as excitations of the Mg 2s2p electrons in the CI expansion. Another way that one can treat this effect without increasing the computational cost is by using core polarization potentials.[18] We have chosen the former procedure. The resulting contraction schemes are the following: for Mg^+ (6s6p) → [4s4p], for Ar (5s5p2d) → [3s3p2d], for Xe (6s6p3d1f) → [3s3p3d1f], for C (4s4p1d) → [2s2p1d] and for O (5s5p2d) → [3s3p2d].

The polarizability of the rare gases plays an important role in the description of the interaction involved in the complexes studied here. A comparison of the polarizabilities computed in this work with experimental polarizabilities gives a measure of the quality of the basis sets. For Ar we have calculated a polarizability 8.90 a_0^3, which is 80% of the experimental value (11.08 a_0^3 [27]) and for Xe 24.36 a_0^3, which is 90% of the experimental value (27.16 a_0^3 [27]).

The molecular orbitals are obtained from SCF calculations followed by improved virtual-orbital (IVO) calculations that optimize the unoccupied orbitals for excited states and configuration interaction.[28] The configurations included in the CI calculations for the Mg^+−RG type complexes resulted from single and double excitations from the *nsn*p orbitals of the RG ($n = 3$ for Ar and $n = 5$ for Xe) and the 3s3p orbitals of Mg or from simultaneous single excitation from 2s2p orbitals of Mg and single excitation from 3s3p orbitals of Mg. The purpose of the Mg^+−CO_2 calculations was for simple qualitative comparisons of the different behavior of the spin−orbit splitting, so only small CI expansions were used. They included single excitations of the Mg(3s) electron to all virtuals.

The computer programs used are from the COLUMBUS suite of programs.[29,30]

3. Results and Discussion

The results for Mg^+−Ar and Mg^+−Xe are shown in Tables 1 and 2 and the potential energy curves calculated in Figures 1 and 2. The interaction between the ion and the RG can be described qualitatively as a charge-induced dipole interaction and a smaller contribution from the dispersion interaction or even the charge-induced quadrupole interaction. One would expect that the Hartree−Fock wave function would describe the charge-induced dipole interaction reasonably well, but for a good description of the dispersion interaction, extensive correlation must be included. By the inclusion of correlation in our calculations for Mg^+−Ar, the dissociation energy was doubled, which implies a significant contribution of dispersion terms to the energy. Only a small part of the dispersion terms could be included in our CI calculations because of the limited capacity of our spin−orbit configuration-interaction program. So even when correlation is included, our dissociation energies are much smaller than the experimental values.[4,6,17]

TABLE 1: Results for Mg^+−Ar[a]

	r_e (Å)	D_e (cm^{-1})	T_e (cm^{-1})
		$X^2\Sigma_{1/2}$	
this work	3.21	539	0
refs 4, 6	2.825[b]	1295 ± 100[c] (1270 ± 165)[c]	0
ref 9	2.854	1041[c]	0
		$A^2\Pi_{1/2}$	
this work	2.54	3363	32 215
refs 4, 6	2.475[e]	5554[c] (5445 ± 165)[c]	31 456[d]
ref 9[f]	2.406	5097[c]	31 585[d]
		$A^2\Pi_{3/2}$	
this work	2.54	3378	32 283
refs 4, 6	2.475[e]	5569 (5460 ± 165)[c]	31 532[d]
ref 9[f]	2.406	5097[c]	31 585[d]
		$B^2\Sigma_{1/2}$	
this work	5.2	97	35 565
refs 4, 6			
ref 9			

[a] Comparison with experimental results from Duncan and coworkers[4,6] and other theoretical work from Bauschlicher and Partridge.[9] Dissociation energies in parentheses are from Le Roy's work.[16] $A_{\Lambda\Sigma}$: 68.0 cm^{-1} (73.9 cm^{-1}). [b] Corresponds to r_0. [c] Corresponds to D_0. [d] Corresponds to ν_{00}. [e] Corresponds to r_5. [f] Corresponds to a weighted average of the two components.

TABLE 2: Results for Mg^+−Xe[a]

	r_e (Å)	D_e (cm^{-1})	T_e (cm^{-1})
		$X^2\Sigma_{1/2}$	
this work	3.31	1494	0
ref 4		4182[b] (3299 ± 1654)[b]	0
		$A^2\Pi_{1/2}$	
this work	2.79	6479	30 051
ref 4		11026[b] (10019 ± 1654)[b]	28 825[c]
		$A^2\Pi_{3/2}$	
this work	2.80	6285	30 329
ref 4		10847[b] (9843 ± 1654)[b]	29 093[c]
		$B^2\Pi_{1/2}$	
this work	4.8	290	36 323
ref 4			

[a] Comparison with experimental results from Duncan and coworkers.[4] Dissociation energies in parentheses are from Le Roy's work.[16] $A_{\Lambda\Sigma}$: 277.6 cm^{-1} (270.4 cm^{-1}). [b] Corresponds to D_0. [c] Corresponds to ν_{00}.

Despite the modest level of agreement with experiment, the dissociation energies and bond lengths show the expected qualitative behavior. The dissociation energy of the excited $^2\Pi$ state is much higher than that of the ground state while the excited $^2\Sigma^+$ state is barely bound. The equilibrium bond distance increases going from the $A^2\Pi$ to the $X^2\Sigma^+$ state and gets even larger for the $B^2\Sigma^+$ state. Going from Ar to Xe, the complex becomes considerably more bound, as one would expect because of the much higher polarizability of Xe. The bond lengths for the Xe complex are longer because of its larger size.

The excitation energies ($X^2\Sigma^+ \rightarrow A^2\Pi$) are less dependent on electron correlation and are in much better agreement with experimental and other theoretical results. Their behavior is as expected according to the different degrees of binding for the different states and the different rare gases. The atomic excitation ($^2S_{1/2} \rightarrow {}^2P_{1/2}$) for Mg^+ that we calculate is 35 052 cm^{-1}. The excitation energies ($X^2\Sigma^+_{1/2} \rightarrow A^2\Pi_{1/2}$) for Mg^+−

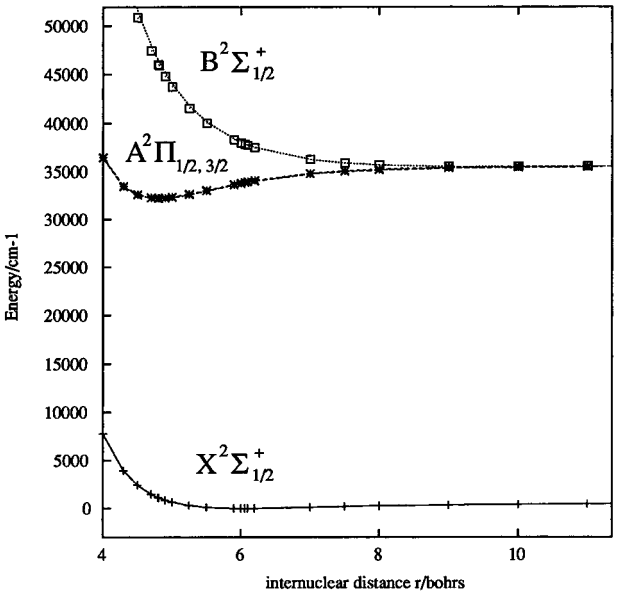

Figure 1. Potential-energy curves for the $X^2\Sigma_{1/2}$, $A^2\Pi_{1/2,3/2}$, and $B^2\Sigma_{1/2}$ states of Mg^+-Ar. The zero of the energy is set to the minimum of the ground state.

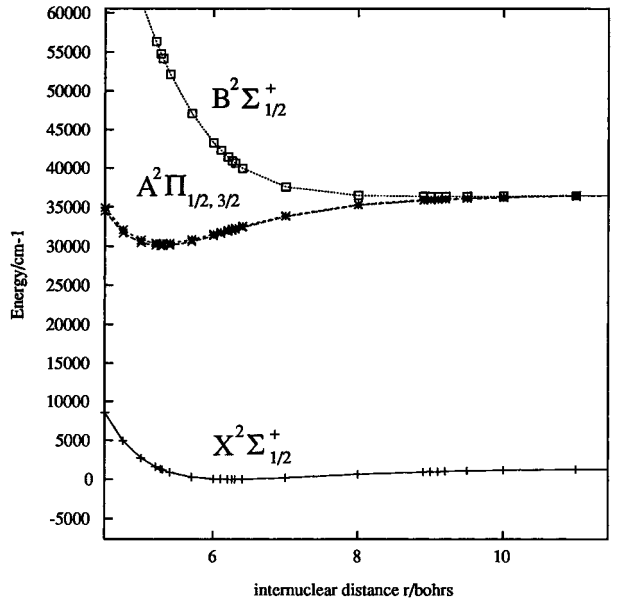

Figure 2. Potential-energy curves for the $X^2\Sigma_{1/2}$, $A^2\Pi_{1/2,3/2}$, and $B^2\Sigma_{1/2}$ states of Mg^+-Xe. The zero of the energy is set to the minimum of the ground state.

Ar and Mg^+-Xe are red-shifted (32 215 and 30 051 cm^{-1}, respectively), showing again that the $^2\Pi$ state is more bound than the ground state and increases going from Ar to Xe. The excitation energies for $X^2\Sigma^+ \rightarrow B^2\Sigma^+$ are blue-shifted (35 565 and 36 323 cm^{-1} for the Ar and Xe complexes, respectively), showing the weaker bonding in the $B^2\Sigma^+$ state compared to the bonding in the ground state. There are no experimental or other theoretical results for the $B^2\Sigma^+$ state.

An important characteristic of these complexes is the behavior of the spin−orbit splitting for the two components ($\Omega = {}^1/_2$, $\Omega = {}^3/_2$) of the $A^2\Pi$ state. If A_{LS} is the atomic spin−orbit coupling constant ($H^{SO} = A_{LS}\,\mathbf{L}\cdot\mathbf{S}$) of Mg^+, then the spin−orbit splitting for the two components of the ^2P state is ${}^3/_2 A_{LS}$. For the molecule, the energy difference between $\Omega = {}^3/_2$ and $\Omega = {}^1/_2$ is $A_{\Lambda\Sigma}$ where $A_{\Lambda\Sigma}$ is the molecular spin−orbit coupling constant ($\langle H^{SO}\rangle = A_{\Lambda\Sigma}\,\Lambda\Sigma$). In the simplest model, these two constants are equal, and the spin−orbit splitting for the complexes should

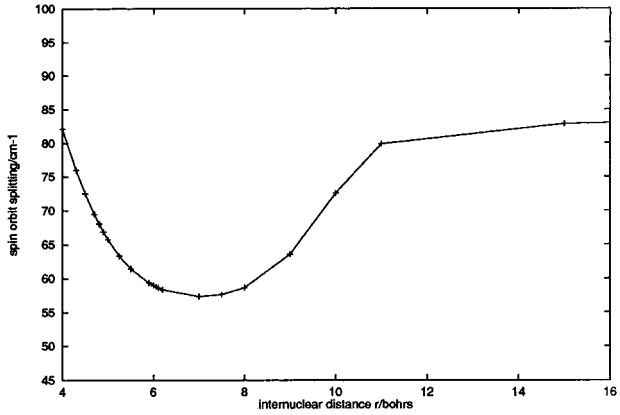

Figure 3. Internuclear-distance dependence of the spin−orbit splitting ($E(^2\Pi_{3/2}) - E(^2\Pi_{1/2})$) for Mg^+-Ar.

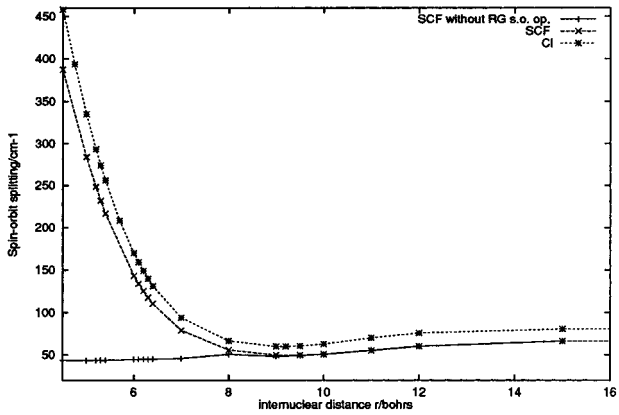

Figure 4. Internuclear-distance dependence of the spin−orbit splitting ($E(^2\Pi_{3/2}) - E(^2\Pi_{1/2})$) for Mg^+-Xe. Plots obtained from CI calculations, from SCF calculations, and from SCF excluding the spin−orbit operator of the RG show that correlation is not responsible for the increase of the spin−orbit splitting at closer distances and that the RG plays an essential role.

be ${}^2/_3$ of the atomic spin−orbit splittings. In our calculations the atomic spin−orbit splitting is 85.5 cm^{-1}, so the expected spin−orbit splitting for the complexes is about 57 cm^{-1}.

For both RG complexes we calculate values higher than this expected value. For Mg^+-Ar, the spin−orbit splitting is 68.0 cm^{-1}, while for Mg^+-Xe it is 277.6 cm^{-1} at the equilibrium distance of the $A^2\Pi$ state. Also, the spin−orbit splitting changes as a function of the internuclear distance, as can be seen in Figures 3 and 4. At the dissociation limit it approaches the atomic value. As the atoms approach each other, it decreases, going to the molecular limit that corresponds to the expected value of 57 cm^{-1}. But before they reach their equilibrium distance, it starts increasing again, doing so at a much faster rate for the Xe complex than for the Ar complex.

This behavior has been observed in the experimental study of these systems and in many similar systems, and the short-range behavior has particularly been the focus of discussion. Neutral van der Waals complexes of alkali metals with rare-gas atoms have the same electronic configuration, and their excited $^2\Pi$ state reveals the same behavior. For Na−RG the expected spin−orbit splitting is 11.5 cm^{-1}, but the values found are 20, 50, and 110 cm^{-1} for RG = Ar, Kr, and Xe respectively.[31] There have been many attempts to explain this phenomenon. An early suggestion was that the RG perturbs the 2p core electrons of the metal, and since the spin−orbit constant for those is much higher than the spin−orbit constant for the 3p electrons, that would cause the increase in the spin−

orbit splitting. This suggestion was shown to be unlikely.[32] More recent interpretations state that the RG accounts for the short-range increase. There are different ways that the RG can contribute, and Breckenridge et al.[33] have a detailed discussion of them. One way would be mixing of the M^+−RG($np^5(n+1)p$) configuration where the p-hole character of the rare gas would increase the spin−orbit splitting, but this would give rise to an inverted multiplet, and this is not observed. Another explanation is mixing of M^{2+}−RG($np^6(n+1)p$) configurations. This would give a normal multiplet, but the spin−orbit constant for the $(n+1)p$ orbitals of the rare gas atom is much smaller than that for the np. So an important increase in the spin−orbit splitting of the complex, such as the one observed, is only feasible if a high level of mixing of rare gas $(n+1)p$ character is involved. Recently, Yarkony and Sohlberg[34] have studied this effect in LiAr and LiNe with theoretical calculations. They used CI methods to obtain the nonrelativistic wave functions and first-order perturbation theory for the spin−orbit term. Their interpretation is very similar to ours.

In the above description of the spin−orbit splitting, it was assumed that the atomic spin−orbit coupling constant A_{LS} is equal to the molecular one $A_{\Lambda\Sigma}$. This is true, however, only as long as the π orbital occupied by the single electron has pure Mg $3p\pi$ character.[35] Because of the SCF MO coefficients, it is evident that this is not true. At short distances, there is a substantial mixing of RG $p\pi$ character. The contribution of RG $np\pi$ character is much higher than the contribution of RG $(n+1)p\pi$ character. In a qualitative description, the molecular orbital that describes the valence electron can be expressed as a linear combination of the atomic $p\pi$ orbitals of Mg and the RG. The Mg and RG $p\pi$ orbitals must remain orthogonal as the internuclear distance decreases. Since the Mg $p\pi$ orbital is singly occupied and at higher energy while the RG $p\pi$ orbital is quadruply occupied and at lower energy, it is the Mg $p\pi$ orbital that bears the brunt of the change. In a very simplified approximation, making the Mg $p\pi$ orbital orthogonal to the RG $p\pi$ orbital gives

$$|\pi\rangle = \frac{|3p\pi_{Mg}\rangle - S|np\pi_{RG}\rangle}{\sqrt{1-S^2}}$$

where S is the overlap between the Mg and RG $p\pi$ atomic orbitals. Then, neglecting two-center integrals, $A_{\Lambda\Sigma}$ can be expressed as a linear combination of the atomic spin−orbit parameters for each atom:

$$A_{\Lambda\Sigma} = \frac{\zeta(3p)_{Mg} + S^2\zeta(np)_{RG}}{1-S^2}$$

The atomic spin−orbit parameters of Ar and Xe are much larger than that of Mg, so even a small amount of mixing increases $A_{\Lambda\Sigma}$ significantly.

This mixing of MOs at short range is a simple manifestation of short-range (steric) repulsion and is usually described well even by SCF wave functions. Note that this mixing (distortion) does not imply significant charge transfer. By Mulliken population analysis, the population of this MO on the RG remains zero at all distances.

Curves of the spin−orbit splitting vs internuclear distance at the SCF and CI levels show the same behavior, again indicating that this is not a correlation-sensitive result, aside from core-valence correlation on the Mg. When calculations at the SCF level were carried out excluding the spin−orbit operator for the RG, this behavior disappeared and the spin−orbit splitting stayed constant as the atoms approached each other (Figure 4).

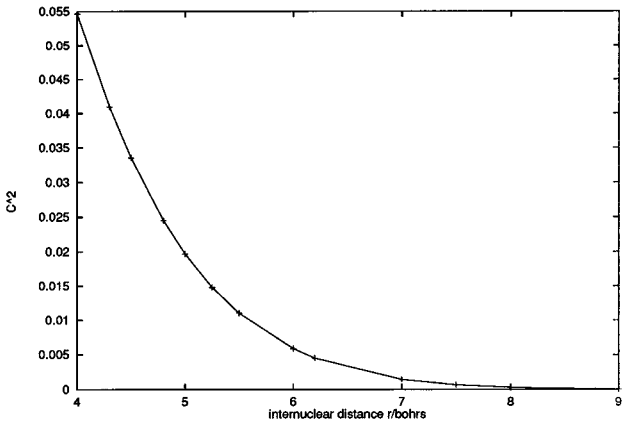

Figure 5. Square of the coefficient of the $3p\pi$ (Ar) in the π MO of the HF wave function.

TABLE 3: Results for Mg^+−CO_2[a]

	r_e Mg^+−C) (Å)	D_e (cm^{-1})	T_e (cm^{-1})
	$X^2\Sigma_{1/2}$		
this work		4959	0
ref 7		5154[b]	0
ref 10	2.10	5736[b]	0
	$A^2\Pi_{1/2}$		
this work		9936	29 921
ref 7		11198[b]	29 625[c]
ref 10[d]	1.99	10 668[b]	30 900[c]
	$A^2\Pi_{3/2}$		
this work		9962	29 965
ref 7			29 681[c]
ref 10[d]	1.99	10 668[b]	30 900[c]

[a] Comparison with experimental results from Duncan and coworkers[7] and other theoretical work from Sodupe et al.[10] $A_{\Lambda\Sigma}$: 44.6 cm^{-1} (56 cm^{-1}). [b] Corresponds to D_0. [c] Corresponds to ν_{00}. [d] Corresponds to a weighted average of the two components.

The contribution of the RG can be obtained from the SCF MOs. The square of the coefficient of the RG($p\pi$) orbital in the π MO is plotted against internuclear distance (Figure 5). As the atoms approach, this contribution gets larger, so the spin−orbit constant gets larger. The behavior of $A_{\Lambda\Sigma}$ is governed by this contribution.

Mg^+−CO_2 is another complex with the same spectrum, so the first excited state is again a $^2\Pi$ state with components with $\Omega = {}^1/_2$ and $\Omega = {}^3/_2$. Experiments on this molecule have shown that the spin−orbit splitting of this state does not display the same behavior as the complexes discussed so far;[7] on the contrary, the value of the spin−orbit splitting is even smaller than the predicted. We carried some low-level calculations in this system, focusing on the spin−orbit aspect of the problem. Results and comparison with other existing experimental and theoretical results are shown in Table 3. We did not optimize the geometries but instead used the optimized geometries of Sodupe et al.[9] A plot of the spin−orbit splitting in a small range is shown in Figure 6. Since core-valence correlation is not included in these calculations, the atomic spin−orbit splitting is only 70 cm^{-1}, so the expected molecular spin−orbit splitting is about 47 cm^{-1}. It is apparent that the spin−orbit is lower than that and decreases as CO_2 approaches Mg^+, but the effect is much smaller than what is experienced by the rare-gas complexes. The Mg^+ $3p\pi$ orbital, in this case, mixes with both the π_u and π_g MOs from CO_2 and therefore has both carbon and oxygen $2p\pi$ character. The atomic spin−orbit parameters

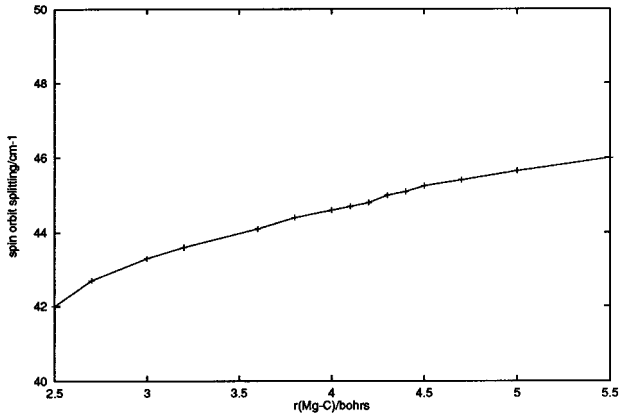

Figure 6. Internuclear-distance dependence of the spin−orbit splitting ($E(^2\Pi_{3/2}) - E(^2\Pi_{1/2})$) for Mg^+-CO_2.

for C(2p) and O(2p) are 29 and 150 cm^{-1}, respectively,[35] which are not extremely different from the Mg^+ parameter (92 cm^{-1}). With three atoms involved, the effect is more complicated and a simple expression was not found, but in general, mixing with C 2pπ will tend to decrease the molecular spin−orbit constant and mixing with O 2pπ to increase it somewhat.

4. Conclusions

The potential energy curves of the $X^2\Sigma^+_{1/2}$, $A^2\Pi_{1/2,3/2}$, and $B^2\Sigma^+_{1/2}$ states of Mg^+-Ar and Mg^+-Xe have been calculated using relativistic core potentials and spin−orbit CI. The charge-induced dipole interaction between the atoms in the complexes is adequately described but not the dispersion interaction. The result is small dissociation energies and large bond distances compared with experimental results. The spin−orbit coupling of the $A^2\Pi$ state and the excitation energies, being much less sensitive to correlation, are described quite efficiently.

The increase in the spin−orbit splitting of the $^2\Pi$ state at short distances in Mg^+-RG is explained as the result of mixing of RG(*n*pπ) character into the Mg^+ 3pπ MO. In Mg^+-CO_2 the same type of mixing is more complicated and causes a small decrease in the spin−orbit splitting.

Acknowledgment. We thank Dr. Michael A. Duncan for suggesting the problem to us and for subsequent helpful discussions. This work was partially supported through Pacific Northwest National Laboratory, Contract 200210, by the U.S. Department of Energy, the Mathematical, Information, and Computational Science Division, High-Performance Computing and Communications program of the Office of Computational and Technology Research. Pacific Northwest National Laboratory is operated by Battelle Memorial Institute under contract DE-AC06-76RL0 1830. Calculations were carried out at the Ohio Supercomputer Center and at the High Performance Computing Research Facility, Mathematics and Computer Science Division, Argonne National Laboratory.

References and Notes

(1) Yeh, C. S.; Pilgrim, J. S.; Willey, K. F.; Robbins, D. L.; Duncan, M. A. *Int. Rev. Phys. Chem.* **1994**, *13*, 231.
(2) Shen, M. H.; Farrar, J. M. *J. Phys. Chem.* **1989**, *93*, 4386.
(3) Shen, M. H.; Farrar, J. M. *J. Chem. Phys.* **1991**, *94*, 3322.
(4) Pilgrim, J. S.; Yeh, C. S.; Berry, K. R.; Duncan, M. A. *J. Chem. Phys.* **1994**, *100*, 7945.
(5) Pullins, S. H.; Scurlock, C. T.; Reddic, J. E.; Duncan, M. A. *J. Chem. Phys.* **1996**, *104*, 7518.
(6) Scurlock, C. T.; Pilgrim, J. S.; Duncan, M. A. *J. Chem. Phys.* **1995**, *103*, 3293.
(7) Yeh, C. S.; Willey, K. F.; Robbins, D. L.; Pilgrim, J. S.; Duncan, M. A. *J. Chem. Phys.* **1993**, *98*, 1867.
(8) Panov, S. I.; Williamson, J. M.; Miller, T. A. *J. Chem. Phys.* **1995**, *102*, 7359.
(9) Bauschlicher, C. W., Jr.; Partridge, H. *Chem. Phys. Lett.* **1995**, *239*, 241.
(10) Sodupe, M.; Bauschlicher, C. W., Jr.; Partridge, H. *Chem. Phys. Lett.* **1996**, *257*, 465.
(11) Bauschlicher, C. W., Jr.; Sodupe, M.; Partridge, H. *J. Chem. Phys.* **1992**, *96*, 4453.
(12) Sodupe, M.; Bauschlicher, C. W., Jr. *Chem. Phys. Lett.* **1992**, *195*, 494.
(13) Bauschlicher, C. W., Jr. *Chem. Phys. Lett.* **1993**, *201*, 11.
(14) Bauschlicher, C. W., Jr.; Sodupe, M. *Chem. Phys. Lett.* **1993**, *214*, 489.
(15) Sodupe, M.; Bauschlicher, C. W., Jr. *Chem. Phys.* **1994**, *185*, 163.
(16) Le Roy, R. J. *J. Chem. Phys.* **1994**, *101*, 10217.
(17) Massick, S.; Breckenridge, W. H. *Chem. Phys. Lett.* **1996**, *257*, 465.
(18) Müller, W.; Flesch, J.; Meyer, W. *J. Chem. Phys.* **1984**, *80*, 3297.
(19) Christiansen, P. A.; Ermler, W. C.; Pitzer, K. S. *Annu. Rev. Phys. Chem* **1988**, *36*, 407.
(20) Pitzer, R. M.; Winter, N. W. *J. Phys. Chem.* **1988**, *92*, 3061.
(21) Pacios, L. F.; Christiansen, P. A. *J. Chem. Phys.* **1985**, *82*, 2664.
(22) Nicklass, A.; Dolg, M.; Stoll, H.; Preuss, H. *J. Chem. Phys.* **1995**, *102*, 8942.
(23) Wallace, N. M.; Blaudeau, J. P.; Pitzer, R. M. *Int. J. Quantum Chem.* **1991**, *40*, 789.
(24) Kendall, R. A.; Dunning, T. H. Jr.; Harrison, R. J. *J. Chem. Phys.* **1992**, *96*, 6796.
(25) Pitzer, R. M. *QCPE* **1990**, *10*, 587.
(26) Blaudeau, J. P.; Brozell, S. R.; Matsika, S.; Zhang, Z.; Pitzer, R. M. Unpublished work.
(27) Kumar, A.; Meath, W. J. *Can. J. Chem.* **1985**, *63*, 1616.
(28) Hunt, W. J.; Goddard, W. A., III. *Chem. Phys. Lett.* **1969**, *3*, 414.
(29) Shepard, R.; Shavitt, I.; Pitzer, R. M.; Comeau, D. C.; Pepper, M.; Lischka, H.; Szalay, P. G.; Ahlrichs, R.; Brown, F. B.; Zhao, J. *Int. J. Quantum Chem. Symp.* **1988**, *22*, 149.
(30) Chang, A. H. H.; Pitzer, R. M. *J. Am. Chem. Soc.* **1989**, *111*, 2500.
(31) Smalley, R. E.; Auerbach, D. A.; Fitch, P. S.; Levy, D. H.; Wharton, L. *J. Chem. Phys.* **1977**, *66*, 3778.
(32) Cooper, D. L. *J. Chem. Phys.* **1981**, *75*, 4157.
(33) Breckenridge, W. H.; Jouvet, C.; Soep, B. *Adv. Met. Semicond. Clusters* **1995**, *3*, 1.
(34) Sohlberg, K.; Yarkony, D. R. *J. Phys. Chem. A* **1997**, *101*, 3166.
(35) Lefebvre-Brion, H.; Field, R. W. *Perturbations in the Spectra of Diatomic Molecules*; Academic: Orlando, FL, 1986.